Requirement of Inducible Nitric Oxide Synthase for Skeletal Muscle Regeneration after Acute Damage

Elena Rigamonti,* Thierry Touvier,† Emilio Clementi,†,‡ Angelo A. Manfredi,*,§ Silvia Brunelli,*,¶,1 and Patrizia Rovere-Querini*,1

Adult skeletal muscle regeneration results from activation, proliferation, and fusion of muscle stem cells, such as myogenic precursor cells. Macrophages are consistently present in regenerating skeletal muscles and participate into the repair process. The signals involved in the cross-talk between various macrophage populations and myogenic precursor cells have been only partially identified. In this study, we show a key role of inducible NO synthase (iNOS), expressed by classically activated macrophages in the healing of skeletal muscle. We found that, after sterile injury, iNOS expression is required for effective regeneration of the tissue, as myogenic precursor cells in the muscle of injured iNOS$^{-/-}$ mice fail to proliferate and differentiate. We also found that iNOS modulates inflammatory cell recruitment: damaged muscles of iNOS$^{-/-}$ animals express significantly higher levels of chemokines such as MIP2, MCP1, MIP-1α, and MCP1, and display more infiltrating neutrophils after injury and a persistence of macrophages at later time points. Finally, we found that iNOS expression in the injured muscle is restricted to infiltrating macrophages. To our knowledge, these data thus provide the first evidence that iNOS expression by infiltrating macrophages contributes to muscle regeneration, revealing a novel mechanism of inflammation-dependent muscle healing. *The Journal of Immunology*, **2013, 190: 1767–1777.**

Skeletal muscle regeneration is an adaptive response to injury or disease that involves the degeneration of damaged myofibers and the activation of quiescent myogenic cells that start to proliferate, differentiate, and fuse, leading to new myofiber formation and reconstitution of a functional contractile apparatus (1). It has become increasingly clear that inflammation is critical for muscle regeneration (2) and that it has to be finely tuned and eventually abated: persistent recruitment of inflammatory cells and/or altered identity of the inflammatory infiltrate are associated with functional impairment of the muscle healing response (3).

Inflammation in acutely damaged muscle is characterized by a rapid and sequential invasion of leukocytes that persists during muscle repair, regeneration, and growth. Infiltrating leukocytes play several roles that have not been completely characterized. Neutrophils contribute to the early muscle membrane lysis following injury through a superoxide-dependent mechanism and the release of myeloperoxidase (4, 5). Later on, macrophages predominate: they remove necrotic debris and sustain the activation and the fusion of the myogenic precursor cells (6–9). Macrophages that infiltrate the tissue at early stages after damage produce cytokines and chemokines, including TNF-α and MCP-1. At later stages they secrete trophic and anti-inflammatory cytokines, such as insulin-like growth factor 1 (IGF-1) and IL-10, which may sustain myofiber reconstitution. The actual role of the various polarized infiltrating macrophages in the healing of the injured muscle and by which signals they interact to this end with myogenic stem cells has been to date poorly characterized.

NO is a key signaling molecule involved in adult skeletal muscle homeostasis, including its regeneration after injury (10–13). In particular, NO promotes myogenic precursor cell activation and fusion and maintains the size of the pool of myogenic precursor cells in acutely and chronically damaged muscles (14). NO is synthesized from L-arginine by NO synthase (NOS) enzymes. Skeletal muscle expresses the constitutive neuronal NOS (nNOS) (15) and the endothelial NOS isoforms. The expression of the inducible high throughput isoform (inducible NOS [iNOS]) has been reported during embryonic muscle development, whereas in the adult it occurs only in inflamed tissues. Previous studies have shown that inhibition of all NOS isoforms jeopardizes muscle regeneration (16, 17), as expected because of the obligatory role of NO in skeletal muscle biogenesis and function. Likewise, ablation of nNOS in myofibers or its functional impairment, as in Duchenne muscular dystrophy, significantly reduces tissue repair. The specific contribution of iNOS to muscle healing has not been investigated yet. Because iNOS is expressed by specific macrophage populations, understanding its function may shed light on the mechanisms and role of inflammation in muscle repair. It may also

*Division of Regenerative Medicine, Stem Cells and Gene Therapy, San Raffaele Scientific Institute, 20132 Milan, Italy; †Eugenio Medea Scientific Institute for Research, Hospitalization and Health Care, 23842 Bosisio Parini, Lecco, Italy; ‡Unit of Clinical Pharmacology, National Research Council, Department of Biomedical and Clinical Sciences Luigi Sacco, Institute of Neuroscience, "Luigi Sacco" University Hospital, University of Milan, 20157 Milan, Italy; §Vita-Salute University, 20132 Milan, Italy; and ¶Dipartimento Scienze della Vita, Milano-Bicocca University, 20135 Milan, Italy

[1]S.B. and P.R.-Q. contributed equally to this article.

Received for publication October 18, 2012. Accepted for publication December 7, 2012.

This work was supported by the Italian Ministry of Health (Fondo per Gli Investimenti della Ricerca di Base-IDEAS to P.R.-Q. and Ricerca Finalizzata to A.A.M. and E.C.), the European Community's Seventh Framework Programme (Project ENDOSTEM, Grant Agreement 241440 to S.B., E.C., and P.R.-Q.), the Association Francaise contre les Myopathies (Grant 15440 to P.R.-Q. and S.B.), the Associazione Italiana Ricerca sul Cancro (to E.C.), and the Ministero dell'Istruzione, dell'Universita' e della Ricerca (to A.A.M. and S.B.).

Address correspondence and reprint requests to Dr. Patrizia Rovere-Querini, DIBIT 3A1, San Raffaele Scientific Institute, Via Olgettina 58, 20132 Milan, Italy. E-mail address: rovere.patrizia@hsr.it

The online version of this article contains supplemental material.

Abbreviations used in this article: CSA, cross-sectional area; CTX, cardiotoxin; IGF-1, insulin-like growth factor 1; iNOS, inducible NO synthase; nNOS, neuronal NOS; NOS, NO synthase; PFA, paraformaldehyde; TA, tibialis anterior.

add relevant information on the pathophysiology of muscle also beyond repair, in those conditions such as cachexia and sarcopenia, in which iNOS is expressed.

In this study, we demonstrate that iNOS expression is restricted to macrophages in the injured muscle and that iNOS expression controls the homeostatic response to sterile injury by regulating myogenic precursor cell function and shaping the inflammatory infiltrate. To our knowledge, these data provide the first evidence that iNOS-expressing macrophages play a nonredundant role in the skeletal muscle repair after injury, revealing a novel mechanism of inflammation-dependent muscle healing.

Materials and Methods

Mice

Wild-type C57BL/6 mice (iNOS$^{+/+}$) were purchased from Charles River Laboratories (Calco, Italy), and mice carrying null mutation for iNOS (B6.129P2-*Nos2*^{tm1Lau}/J mice, iNOS$^{-/-}$) were purchased from The Jackson Laboratory (Bar Harbor, ME). Null mutation of iNOS was confirmed by PCR using an upstream primer that was common for both wild-type and mutant DNA (5′-ACATGCAGAATGAGTACCGG-3′), a wild-type downstream primer (5′-TCAACATCTCCTGGTGGAAC-3′), and a downstream primer for the neomycin cassette (5′-AATATGCGAAGTGGACCTCG-3′). All procedures were performed in the animal facility of San Raffaele Scientific Institute in accordance with European Union guidelines and with the approval of the Institutional Ethical Committee.

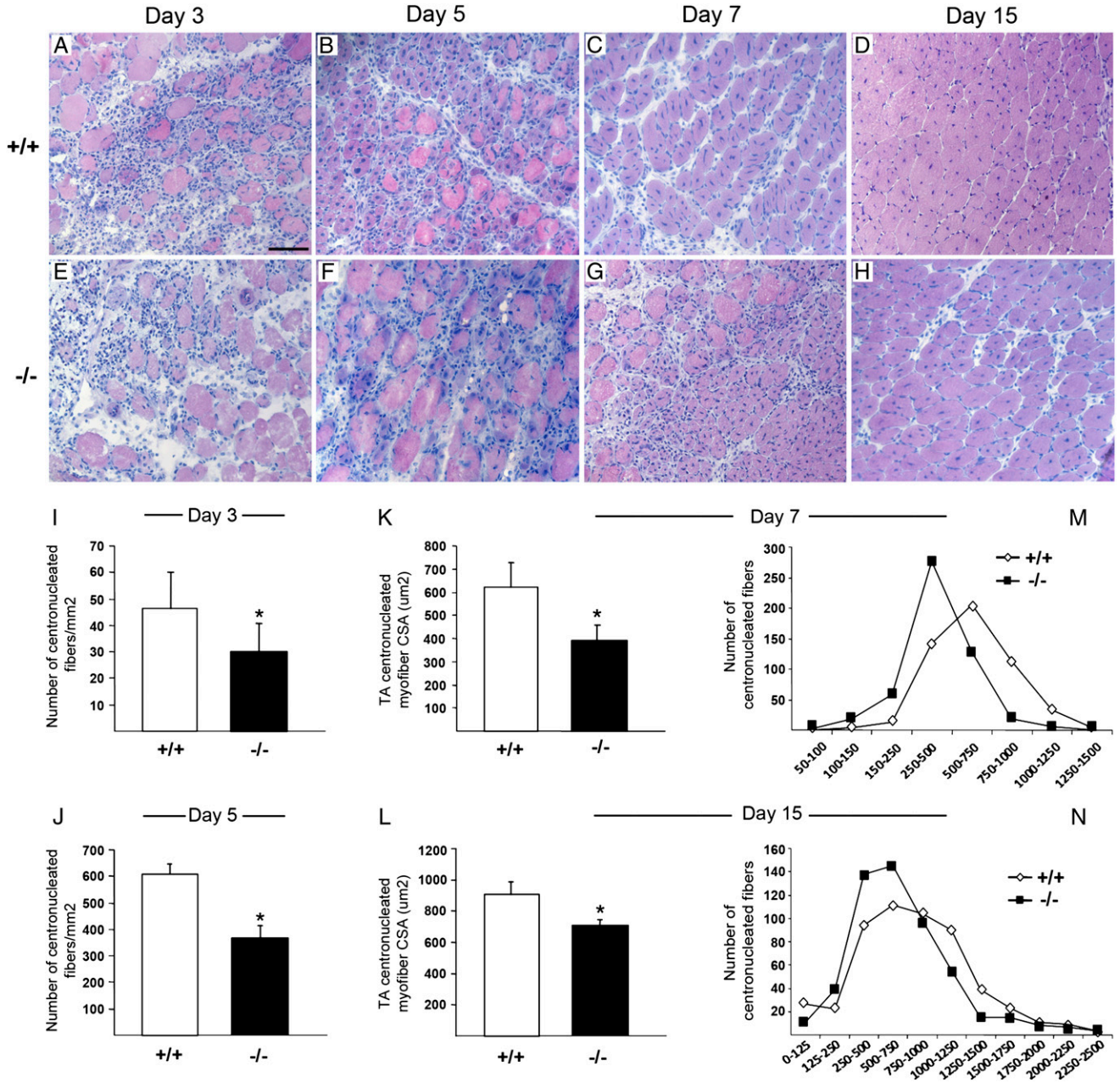

FIGURE 1. iNOS is required for normal muscle regeneration after injury. (**A**–**H**) Representative images of TA muscle cross-sections from 2-mo-old iNOS$^{+/+}$ and iNOS$^{-/-}$ mice at 3 (A, E), 5 (B, F), 7 (C, G), and 15 (D, H) d post-CTX injury, stained for H&E, original magnification ×20. Scale bar, 50 μm. (**I** and **J**) Quantification of the number of centrally nucleated myofibers per mm^2 in iNOS$^{+/+}$ and iNOS$^{-/-}$ regenerating muscles at 3 (I) and 5 (J) d after injury ($n = 5$ mice per genotype). (**K** and **L**) Median CSA of myofibers from regenerating iNOS$^{+/+}$ and iNOS$^{-/-}$ TA muscles at 7 (K) and 15 (L) d postinjury. Data pooled from >750 fibers from $n = 5$ mice per genotype. (**M** and **N**) Frequency histogram showing the distribution of myofiber CSA in the TA muscles from iNOS$^{+/+}$ and iNOS$^{-/-}$ mice at 7 (M) and (N) 15 d postinjury. Bars indicate the mean ± SD. *$p < 0.05$ versus iNOS$^{+/+}$.

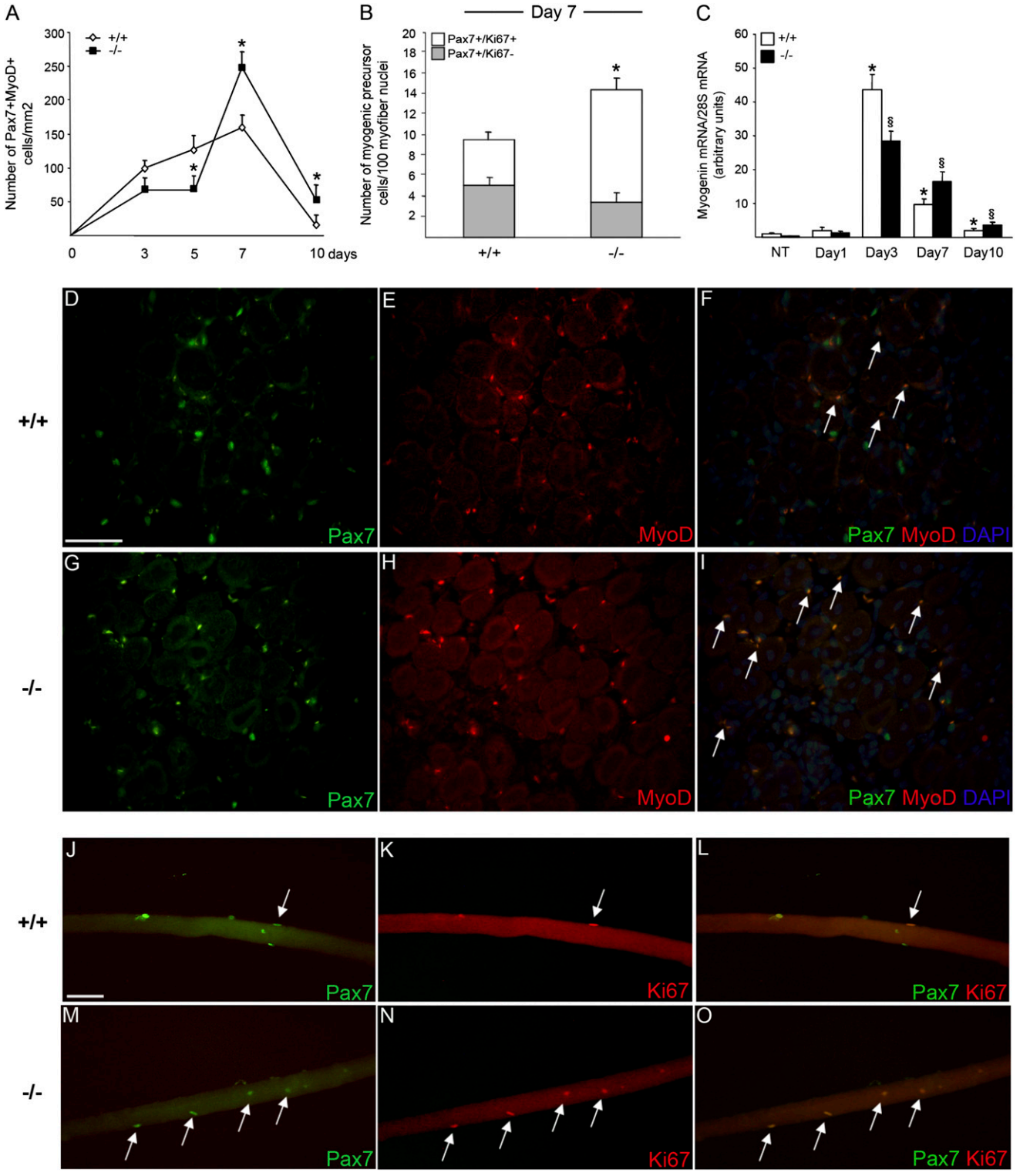

FIGURE 2. iNOS$^{-/-}$ mice display impaired myogenic precursor cell activation after muscle injury. (**A**, **D**–**I**) Immunofluorescence (IF) staining for Pax7 and MyoD on TA muscle sections from iNOS$^{+/+}$ and iNOS$^{-/-}$ mice at days 3, 5, 7, and 10 after CTX injection. (A) Quantification of the number of double-positive Pax7^{+}MyoD^{+} myogenic precursor cells on serial TA sections. Values shown are the results of experiments on three animals per group, mean ± SEM. *$p < 0.05$ versus iNOS$^{+/+}$. (D–I) Representative images of IF on TA sections from iNOS$^{+/+}$ and iNOS$^{-/-}$ mice 7 d after CTX injury, using Abs specific for Pax7 (green; D, G) and MyoD (red; E, H). The superimposed images (overlay) of Pax7 and MyoD staining are shown (F, I) with the addition of Hoechst staining for nuclei. Representative double-positive Pax7^{+}MyoD^{+} myogenic precursor cells are indicated by arrows. Original magnification ×40. Scale bar, 50 μm. (**B**, **J**–**O**) Single muscle fibers were isolated from gastrocnemius muscles of 2-mo-old iNOS$^{+/+}$ and iNOS$^{-/-}$ mice 7 d after injury. Myogenic precursor cells were coimmunostained for Pax7 and Ki67 using a double IF procedure. (B) Histogram representing the number of quiescent Pax7^{+}Ki67^{-} and activated double-positive Pax7^{+}Ki67^{+} myogenic precursor cells on iNOS$^{+/+}$ and iNOS$^{-/-}$ single myofibers. Data are expressed as mean ± SEM, *$p < 0.05$ versus iNOS$^{+/+}$, and normalized for myofiber nuclei number. Results are from at least 50 fibers for each experiment, $n = 3$ per genotype. (J–O) Representative images of iNOS$^{+/+}$ and iNOS$^{-/-}$ single fiber-associated myogenic precursor cells stained for Pax7 (green; J, M) and Ki67 (red; K, N) using a double IF procedure. The superimposed images of Pax7 and Ki67 staining are shown (L, O), and representative double-positive proliferating myogenic (*Figure legend continues*)

Acute muscle damage

iNOS$^{+/+}$ and iNOS$^{-/-}$ C57BL/6 mice were anesthetized and subsequently injected with cardiotoxin (CTX; *Naja mossambica mossambica*, Sigma-Aldrich; 50 μl, 15 μM for tibialis anterior [TA] muscles, 50 μM for quadriceps muscles, or 25 μM for gastrocnemius muscles). Mice were sacrificed at 1, 3, 5, 7, 10, and 15 d after injury. Injured muscles were collected and snap frozen in liquid nitrogen for RNA and protein analyses. For histology, muscles were collected and directly frozen in liquid nitrogen-cool isopentane or fixed before in 4% paraformaldehyde (PFA) and immersed sequentially in 10, 20, 30% sucrose.

Retrieval and purification of muscle-infiltrating inflammatory leukocytes

Infiltrating cells were retrieved from damaged muscles at days 1, 3, 5, 7, and 10 after sterile injury. Muscles were dissociated by enzymatic digestion with collagenase type V (Sigma-Aldrich; 0.5 mg/ml) and dispase (Invitrogen; 3.5 mg/ml) at 37°C for 40 min. Infiltrating cells were further purified by magnetic cell sorting using CD11b-conjugate beads (Milteny Biotec) and processed for protein or RNA extraction. The purity of the retrieved cell population, as verified by flow cytometry using a FACS CANTO (BD Pharmingen) and the Flow Jo Software (Tree Star) after incubation with a PerCP-conjugated anti-CD45 mAb (BD Pharmingen) and allophycocyanin-conjugated anti-CD11b mAb (Clone BD Biosciences), was routinely >92%.

RNA extraction and quantitative real-time PCR analysis

Total RNA was extracted from muscles or from purified muscle-infiltrating CD11b^{+} cells using TRIzol reagent (Invitrogen), following manufacturer's recommendations. Total RNA (1 μg) was reverse transcribed with random hexameric primers and MultiScribe reverse transcriptase (Applied Biosystems), as described (18). cDNAs were quantified by quantitative real-time PCR on a MX 3000 apparatus (Stratagene) using specific primers for Myogenin (5′-GACATCCCCCTATTTCTACCA-3′ forward; 5′-GTCCCCAGTCCCTTTTCTTC-3′ reverse), iNOS (5′-AGCCAAGCCCTCACCTACTT-3′ forward; 5′-TCTCTGCCTATCCGTCTCGT-3′ reverse), nNOS (5′-CTCACCCCGTCCTTTGAGTA-3′ forward; 5′-GGTCGCTTTGACTCTCTTGG-3′ reverse), endothelial NOS (5′-GACCCTCACCGCTACAACAT-3′; 5′-CTGGCCTTCTGCTCATTTTC-3′ reverse), IGF-1 (5′-GTGTGGACCGAGGGGCTTTTACTTC-3′ forward; 5′-GCTTCAGTGGGGCACAGTACATCTC-3′ reverse), IL-10 (5′-ATTTGAATTCCCTGGGTGAGAAG-3′ forward; 5′-CACAGGGGAGAAATCGATGACA-3′ reverse), TNF-α (5′-TCCCAGGTTCTCTTCAAGGGA-3′ forward; 5′-GGTGAGGAGCACGTAGTCGG-3′ reverse), MIP-1α (5′-CTGCCCTTGCTGTTCTTCTC-3′ forward; 5′-CCCAGGTCTCTTTGGAGTCA-3′ reverse), MIP2 (5′-AGTGAACTGCGCTGTCAATG-3′ forward; 5′-TTCAGGGTCAAGGCAAACTT-3′ reverse), MCP3 (5′-AATGCATCCACATGCTGCTA-3′ forward; 5′-CTTTGGAGTTGGGGTTTTCA-3′ reverse), MCP1 (5′-CCCAATGAGTAGGCTGGAGA-3′ forward; 5′-GCTAAGACCTTAGGGCAGA-3′ reverse), 28S (5′-AAACTCTGGTGGAGGTCCGT-3′ forward; 5′-CTTACCAAAAGTGGCCCACTA-3′ reverse), cyclophilin A (5′-CATACGGGTCCTGGCATCTTGTCC-3′ forward; 5′-TGGTGATCTTCTTGCTGGTCTTGC-3′ reverse). PCR amplification was performed in a volume of 20 μl containing 1 μl cDNA, 100 nmol/L of each primer, 4 mmol/L $MgCl_2$, the Brillant Quantitative PCR Core Reagent Kit mix, and SYBR Green 0.33×. The conditions were 95°C for 10 min, followed by 40 cycles of 30 s at 95°C, 30 s at 55°C, and 30 s at 72°C. The housekeeping gene 28S or cyclophilin A was used for normalization.

Western blot analysis

Skeletal muscle and purified CD11b^{+} infiltrating cells were lysed in 10 mM Tris (pH 8.0), 150 mM NaCl, 1% Nonidet P40, 0.1% $NaDodSO_4$ (SDS), 10 mM EDTA, and protease inhibitor mixture (Sigma-Aldrich). Lysates were centrifuged at maximum speed for 15 min at 4°C. For Western blot analysis, equal amounts of protein (50 μg) were resolved by SDS-PAGE and transferred onto Immobilon-P (Millipore). After Ponceau S (Sigma-Aldrich) staining, membranes were saturated in 20 mM Tris-HCl (pH 7.6), 150 mM NaCl (TBS) containing 5% nonfat milk, and 0.1% Tween 20. Ags were detected using rabbit polyclonal anti-mouse iNOS (1:400; Cell Signaling), rabbit polyclonal anti-mouse nNOS (1:400; BD Transduction Laboratories), rabbit polyclonal anti-mouse arginase I (1:1,000; Santa Cruz Biotechnology), mouse monoclonal anti–β-actin (1:10,000; Sigma-Aldrich), or mouse monoclonal anti-GAPDH (1:5,000; Sigma-Aldrich) Abs. All Abs were diluted in TBST 5% nonfat milk. Bands were revealed using an ECL detection kit (GE Healthcare Europe).

Histology

Muscle damage and repair were evaluated after H&E staining on 8-μm–thick serial muscle sections. Fiber cross-sectional area (CSA) and central nucleation analyses were carried out on 750–1000 fibers per muscle by using Image J software (http://rsbweb.nih.gov/ij/). For immunofluorescence, sections were blocked with 5% BSA and 0.1% Triton in PBS before incubation with rat polyclonal anti-CD11b (1:50; BD Pharmingen) and rabbit polyclonal anti-iNOS Abs (1:100; Assay Designs) to identify macrophages, or mouse monoclonal anti-Pax7 (1:2; Developmental Studies Hybridoma Bank) and rabbit polyclonal anti-MyoD Abs (1:25; Santa Cruz Biotechnology) to identify myogenic precursor cells. Appropriate Alexa Fluor (Alexa 488 or Alexa 594)-conjugated Abs (1:500; Invitrogen) were used as second-step reagents. Specimens were counterstained with Hoechst 33342 (Molecular Probes) and analyzed using a Nikon Eclipse 55i microscope (Nikon). Images were captured with Digital Sight DS-5 M digital camera (Nikon) using Lucia G software (Laboratory Imaging). Pax7- and MyoD-expressing myogenic precursor cells were quantified using ImageJ software. Immunohistochemistry was performed on muscle sections fixed with 4% PFA treated with 0.3% H_2O_2 and with an avidin-biotin blocking kit (Vector Laboratories), according to the manufacturer's instructions. Tissue sections were stained respectively with rat anti-mouse Ly-6G (1:100; BioLegend) for neutrophils or rat anti-mouse CD68 mAb (1:100; AbD Serotec), rabbit anti-mouse CD163 mAb (1:200; Santa Cruz Biotechnology), and rat anti-mouse CD206 mAb (1:150; AbD Serotec) for macrophages. Primary Abs were revealed using biotin-conjugated anti-rat (1:300) or anti-rabbit (1:500) IgG (eBiosciences) and HRP streptavidin (Vector Laboratories), and detected using Vector NovaRED substrate kit (Vector Laboratories). Slides were counterstained with hematoxylin and examined with a Nikon Eclipse 55i microscope (Nikon). Parallel slides without primary Abs were identically processed and used as negative controls. Results were quantified using ImageJ software.

Single fiber preparation and immunofluorescence

Gastrocnemius muscles of 2-mo-old iNOS$^{+/+}$ and iNOS$^{-/-}$ mice (three animals of each genotype for experiments) were carefully dissected and digested in 0.1% collagenase type V (Sigma-Aldrich). Individual myofibers were dissociated, as described (14). Microscopic examination was then performed to rule out contamination by capillaries. Myofibers were fixed for 10 min in 4% PFA/PBS (Sigma-Aldrich) within 2 h. Myofibers were subsequently washed with PBS and processed for immunofluorescence using mouse monoclonal anti-Pax7 and/or rabbit anti-mouse Ki67 Abs (1:50; Novocastra, Leica). Fibers were incubated in PBS containing 0.1% Triton X-100 and 10% goat serum for 30 min and then challenged with PBS containing 1% goat serum and the primary Ab overnight at 4°C. Incubation with the second-step reagent was carried out for 1 h at room temperature. Nuclei were counterstained with Hoechst 33342, and samples were mounted on slides using Gel-Mount aqueous mounting medium (Biomeda).

Isolation of primary myoblasts

Primary myoblasts from newborn iNOS$^{+/+}$ and iNOS$^{-/-}$ mice were isolated, as described (19), and plated at clonal density. Cells were propagated in proliferation medium (IMDM supplemented with 20% FBS, 3% chick embryo, 100 U/ml penicillin, 100 μg/ml streptomycin, and 50 μg/ml gentamicin) and subsequently shifted in differentiation medium (IMDM supplemented with 2% horse serum, 100 U/ml penicillin, and 100 μg/ml streptomycin). After 24 and 48 h, cells were fixed with 4% PFA and stained with anti-sarcomeric myosin MF20 mAb (1:2; Developmental Studies Hybridoma Bank). Fusion index was determined as the number of nuclei in sarcomeric myosin-expressing cells with more than two nuclei versus the total number of nuclei.

precursor cells are indicated by arrows. Original magnification ×20. Scale bar, 50 μm. (**C**) Time course changes in the expression of myogenin during muscle regeneration. Skeletal muscles from iNOS$^{+/+}$ and iNOS$^{-/-}$ mice were collected immediately before and 1, 3, 7, and 10 d after injection of CTX and totally lysated. mRNA levels of myogenin were quantified by real-time PCR analysis and normalized to 28S mRNA levels. Results are expressed as relative fold changes compared with muscles from undamaged control animals (NT). Values shown are the results of experiments on six animals per group. Statistically significant differences are indicated (ANOVA/*t* test, iNOS$^{-/-}$ versus iNOS$^{+/+}$; $^{\S}p < 0.05$, $^{*}p < 0.05$ versus NT).

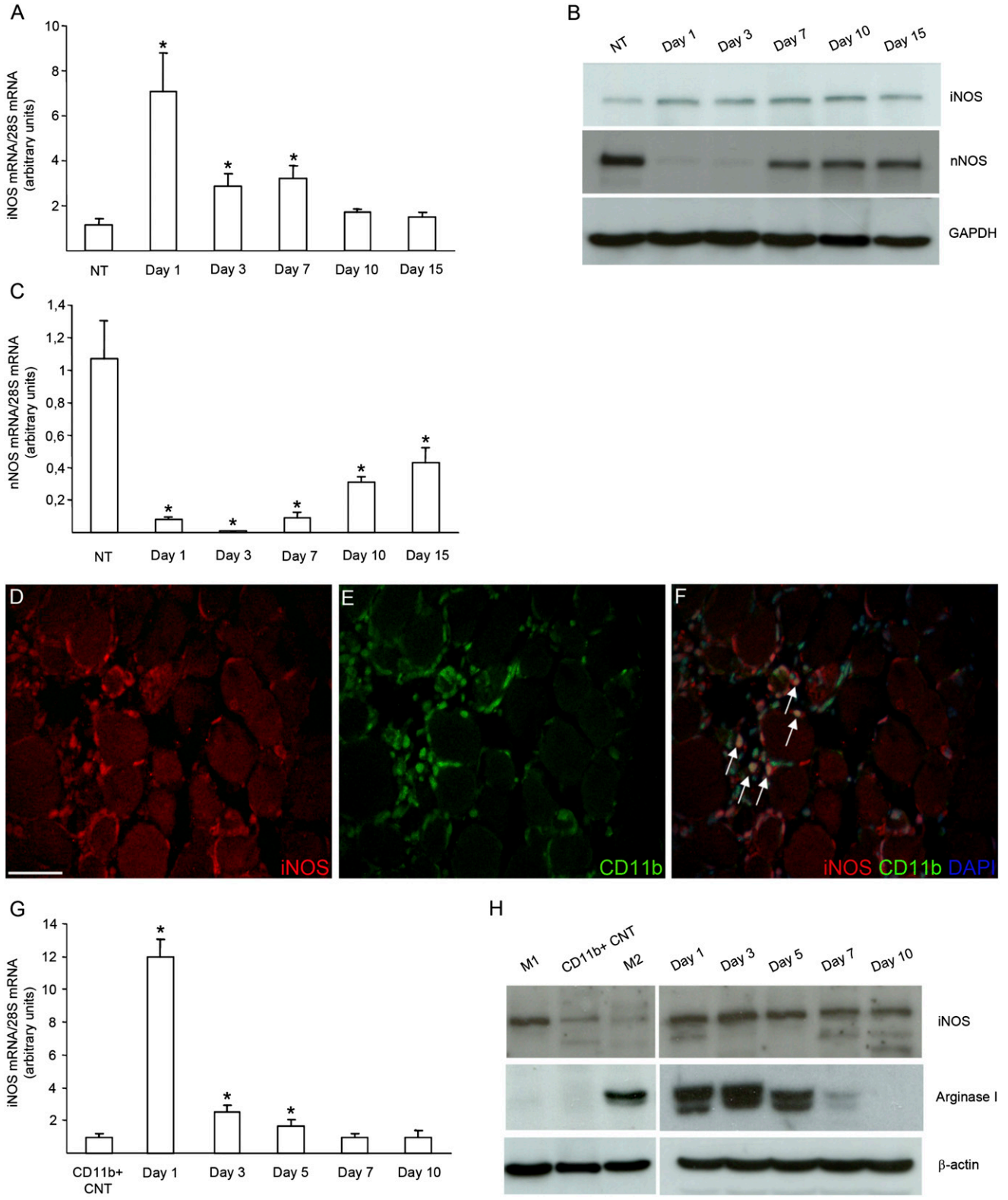

FIGURE 3. iNOS expression is restricted to macrophages in skeletal muscle after acute damage. Quadriceps and TA muscles from 2-mo-old iNOS$^{+/+}$ mice were collected immediately before and 1, 3, 7, 10, and 15 d after CTX injection. Muscles were totally lysated or digested to isolate CD11b^{+} cells by magnetic bead sorting and processed for RNA or protein extraction. (**A** and **C**) Time course changes in the expression of iNOS (A) and nNOS (C) during muscle regeneration were evaluated by real-time PCR. Results were normalized to 28S mRNA levels and expressed as relative fold changes compared with undamaged muscles (NT). Bars indicate the mean ± SEM, $n = 6$. *$p < 0.05$ versus NT. (**B**) Western blot analysis of iNOS and nNOS expression in total healthy muscles and at different time points after CTX injection. Results are representative of five independent experiments. (**D**–**F**) Representative images of IF on TA sections from 2-mo-old iNOS$^{+/+}$ mice 3 d after CTX injury, using Abs specific for iNOS (red; D) and CD11b (green; E). The superimposed images (overlay) of iNOS and CD11b staining are shown (F) with the addition of Hoechst staining for nuclei. iNOS-positive muscle-infiltrating CD11b^{+} macrophages are indicated by arrows. Original magnification ×40. Scale bar, 50 μm. (**G**, **H**) iNOS and arginase I expression was analyzed in CD11b^{+} cells retrieved from peripheral blood (CD11b^{+} CNT) or from muscles 1, 3, 5, 7, and 10 d after CTX injection by real-time PCR (G) (*Figure legend continues*)

Results

iNOS is required for efficient muscle regeneration in vivo

We compared muscles from age-matched iNOS$^{+/+}$ and iNOS$^{-/-}$ mice and found no significant difference in weight (data not shown), morphology (Supplemental Fig. 1A, 1D), and myofiber CSA (Supplemental Fig. 1B, 1C, 1E, 1F). These data indicate that skeletal muscles of iNOS$^{+/+}$ and iNOS$^{-/-}$ mice do not substantially differ in physiological conditions and that iNOS expression is dispensable for the development and the physiology of the healthy tissue. We then investigated the iNOS role in the tissue homeostatic response to sterile injury. TA muscles of 2-mo-old iNOS$^{+/+}$ and iNOS$^{-/-}$ mice were injected with CTX, retrieved 3, 5, 7, and 15 d after damage, and processed for H&E staining (Fig. 1A–H). Myofiber necrosis and massive infiltration of leukocytes and regenerating centrally nucleated myofibers were detectable 3 d after injury (Fig. 1A, 1E). At later time points (7, 15 d), infiltrating cells progressively disappeared from the injured muscles of iNOS$^{+/+}$ mice, and the diameter of regenerating fibers progressively increased (Fig. 1C, 1D). In contrast, inflammatory cells persisted in the injured tissues of iNOS$^{-/-}$ mice and were preferentially distributed in the areas surrounding necrotic myofibers (Fig. 1G, 1H). Regenerating myofibers were significantly less in iNOS$^{-/-}$ injured muscles (Fig. 1I, 1J) and smaller, as indicated by the CSA analyses (Fig. 1K–N).

iNOS controls myogenic precursor cell early activation

We have investigated the function of myogenic precursor cells in iNOS$^{+/+}$ versus iNOS$^{-/-}$ mice by analyzing the expression of specific myogenic markers. Pax7 is a transcription factor expressed by quiescent and activated, but not differentiating, myogenic precursor cells. Upon activation, myogenic precursor cells start proliferating, giving rise to Pax7^{+}MyoD^{+} cells, which are committed to differentiation. Myogenin is a transcription factor only expressed by differentiating myogenic cells.

A progressive increase in the number of Pax7^{+} myogenic precursor cells that express the activation marker MyoD was detectable by immunofluorescence in tissues of iNOS$^{+/+}$ mice during the first 7 d after injury, reflecting myogenic precursor cell activation and proliferation (Fig. 2A, 2D–F). By contrast, the number of activated Pax7^{+}/MyoD^{+} myogenic precursor cells within damaged areas of iNOS$^{-/-}$ mice was initially lower while increasing at later time points (7, 10 d) (Fig. 2A, 2G–I). Indeed, at day 7 after damage, the number of myofiber-associated proliferating Pax7^{+}/Ki67^{+} myogenic precursor cells in iNOS$^{-/-}$ mice was significantly higher than in iNOS-expressing counterparts (Fig. 2B, 2J–O). Moreover, the expression of myogenin, a marker of myogenic precursor cell differentiation, was significantly lower at day 3, while increasing at later time points (Fig. 2C). All together these data indicate a role of iNOS in the early response of myogenic precursor cells to muscle injury in vivo, enabling them to swiftly undergo activation, proliferation, and later on differentiation. Of importance, single myofibers isolated from iNOS$^{+/+}$ and iNOS$^{-/-}$ muscles before injury had similar numbers of associated Pax7^{+}/MyoD^{-} quiescent myogenic precursor cells (Supplemental Fig. 2A–C), indicating that the myogenic precursor cell pool in the two mouse lines does not substantially differ under physiological conditions. Indeed, myogenic precursor cells isolated from iNOS$^{+/+}$ or iNOS$^{-/-}$ mice expanded with similar kinetics in vitro and fused with similar efficiency (Supplemental Fig. 2D–F), making unlikely that the phenotype we observed was due to a myogenic precursor cell-autonomous defect. Because myogenic precursor cells do not express iNOS (data not shown), the differences in iNOS-expressing and deficient mice appear to depend on specific iNOS-dependent signals originating during muscle repair by other cells.

Macrophages express iNOS in the injured/regenerating skeletal muscle

iNOS mRNA and protein were barely detectable by real-time PCR and Western blot analysis in healthy skeletal muscle (Fig. 3A, 3B). iNOS expression increased 24 h after injury and persisted at 3 and 7 d, to decrease at later time points (Fig. 3A, 3B). nNOS had a virtually opposite expression profile compared with iNOS; although highly expressed in the healthy tissue (Supplemental Fig. 1G), where it is the most abundant NOS isoform, it disappeared after muscle injury to become again detectable only at the later time points (Fig. 3B, 3C). We then characterized the pattern of iNOS expression by immunofluorescence in the injured and regenerating tissue. We found that iNOS expression was restricted to inflammatory leukocytes, identified by the expression of the CD11b lineage marker (Fig. 3D–F). Moreover, we purified CD11b^{+} leukocytes by immunomagnetic bead sorting before and at various time points after injury: iNOS was virtually absent before injury in blood CD11b^{+} cells that represent the likely precursors of muscle-infiltrating phagocytes, which in contrast abundantly expressed the molecule 1, 3, and 5 d after damage (Fig. 3G, 3H). These data identify phagocytes—initially neutrophils and from day 3 macrophages (data not shown)—as the iNOS-expressing cells and indicate that iNOS expression depends on specific cues associated to the injured tissue. A similar expression profile was observed for arginase 1, which uses the same substrate of NOS, L-arginine (Fig. 3H).

iNOS shapes the recruitment of leukocytes and the production of cytokines in the injured and regenerating muscle

Muscle injury and healing encompass the recruitment of inflammatory cells (20). We analyzed the role of iNOS-expressing macrophages in shaping the inflammatory response during muscle healing at 1, 3, 7, and 15 d after CTX injection. At day 1 after injury, neutrophil infiltration was significantly higher in the injured muscle of iNOS$^{-/-}$ than in those of iNOS$^{+/+}$ mice, as assessed by the immunohistochemical analysis of the neutrophil surface marker Ly-6G (Fig. 4A–C), thus indicating that iNOS expression quenches the infiltration of neutrophils at sites of injury. Infiltration by CD68^{+} macrophages was significantly more important in muscles of iNOS$^{+/+}$ mice than iNOS$^{-/-}$ littermates at 1 and 3 d after injury (Fig. 4C, 4D, 4G, 4J). This effect was transient because 7 and 15 d after injury macrophages disappeared from the tissues of wild-type animals while increasing in iNOS$^{-/-}$ muscles (Fig. 4C, 4H, 4I, 4K, 4L). A fraction of CD68^{+} macrophages also expressed the haptoglobin/hemoglobin scavenger receptor, CD163, and the mannose receptor, CD206, two markers of alternatively activated cells (data not shown). Interestingly, iNOS did not detectably influence the expression of these markers, as assessed by quantitative analyses of muscle serial sections (Fig. 4E, 4F).

and by Western blot analysis (H). (G) mRNA levels of iNOS were normalized to 28S mRNA levels and expressed as relative fold changes compared with CD11b^{+} cells retrieved from peripheral blood (CD11b^{+} CNT). Bars indicate the mean ± SD, $n = 3$ mice per three independent experimental cohorts. *$p <$ 0.05 versus CD11b^{+} CNT. (H) Results are representative of three independent preparations. In vitro polarized IFN-γ (M1) and IL-10 (M2) macrophages were used as internal control.

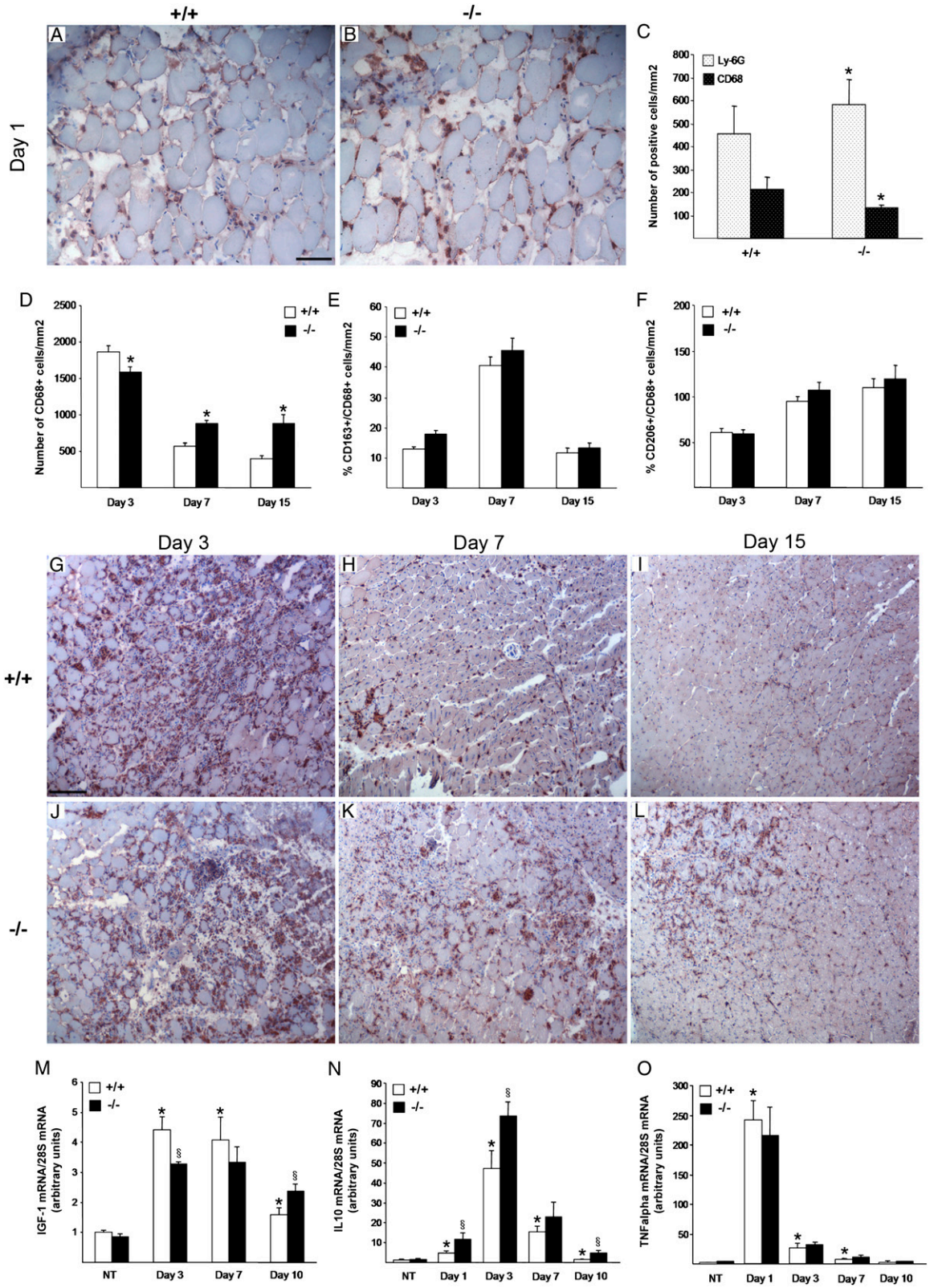

FIGURE 4. Muscle inflammatory infiltrate is perturbed in iNOS$^{-/-}$ after acute damage. Muscle infiltration of neutrophils and macrophages 1 d after CTX injection was detected by immunohistochemical (IHC) staining with specific Abs respectively for Ly-6G (**A**–**C**) and CD68 (C) on TA muscle sections of iNOS$^{+/+}$ and iNOS$^{-/-}$ mice. (A and B) Images are representative of four independent experiments. Original magnification ×20. Scale bar, 50 μm. (C) Quantification of the number of positive cells on serial TA sections. Values shown are the results of experiments on four animals per group, mean ± SD, *$p < 0.05$ versus iNOS$^{+/+}$. (**D**–**L**) Macrophage infiltration in muscle sections of iNOS$^{+/+}$ and iNOS$^{-/-}$ mice at days 3, 7, and 15 from CTX injection. The number of CD68 (D)-, CD163 (E)-, and CD206 (F)-positive cells was assessed on serial TA muscle section at the indicated time points. Values shown are the results of experiments on four animals per group, mean ± SEM, *$p < 0.05$ versus iNOS$^{+/+}$. (G–L) Representative images of TA muscle cross-sections from 2-mo-old iNOS$^{+/+}$ and iNOS$^{-/-}$ mice at 3 (G, J), 7 (H, K), and 15 (I, L) days post-CTX injury, immunostained for CD68. Original magnification ×10. Scale bar, 100 μm. (**M**–**O**) Time course changes in expression of IGF-1, IL-10, and TNF-α during muscle regeneration. Muscles from (*Figure legend continues*)

To investigate the mechanism through which iNOS acts, we analyzed the expression of selected growth factors, cytokines, and chemokines that have been associated with the preferential tissue infiltration by inflammatory cells. Real-time PCR analyses revealed that the expression of IGF-1 in $iNOS^{+/+}$ muscles was upregulated after injury (3, 7 d) to decrease at later time points (day 10), whereas in $iNOS^{-/-}$ counterparts IGF-1 mRNA increase was significantly lower, but persistent (Fig. 4M). IL-10 expression was increased between day 1 and 10 after injury in the muscles of both $iNOS^{+/+}$ and $iNOS^{-/-}$ mice. IL-10 mRNA levels were always significantly higher in $iNOS^{-/-}$ injured muscles (Fig. 4N). No difference was observed in TNF-α expression between $iNOS^{+/+}$ and $iNOS^{-/-}$ muscles (Fig. 4O).

The expression of (MIP)-1α, MIP2, MCP1, and MCP3 was upregulated in injured muscles of $iNOS^{+/+}$ mice at days 1 and 3 after damage (Fig. 5A–D), to abate at later time points. Expression of MIP2, a potent chemoattractant and activator of neutrophils, was significantly higher in $iNOS^{-/-}$ muscles (Fig. 5A) and infiltrating leukocytes (Fig. 5E). Early after injury, $iNOS^{-/-}$ muscles and leukocytes displayed less MCP1 mRNA levels (Fig. 5B, 5F). Expression of MIP-1α and MCP3, involved in both macrophage and neutrophil recruitment, was significantly higher in $iNOS^{-/-}$ injured muscles (Fig. 5C, 5D) and infiltrating $CD11b^{+}$ leukocytes (Fig. 5G, 5H) at all the analyzed time points. These results suggest that macrophage iNOS acts as an early homeostatic regulator of inflammatory leukocyte recruitment.

Discussion

The regeneration of injured muscle involves a complex and tightly regulated interaction between inflammatory cells recruited into the injured tissue and myogenic precursor cells. Macrophages predominate in damaged and regenerating muscle. They have been known for a long time to be associated with skeletal muscle injury (21, 22), and in vivo studies have unequivocally shown that they actually participate in the tissue repair process (7, 18, 23–28). Although several molecules have been identified to be dispensable for muscle regeneration, the overall array of signals that macrophages deliver in the tissue and the hierarchy among them is far from being elucidated.

To our knowledge, the present study provides the first evidence that iNOS contributes to muscle regeneration after injury, revealing a novel mechanism of inflammation-dependent muscle healing. We found that injured muscles of iNOS-deficient mice display impaired muscle regeneration, as indicated by decreased number and size of new regenerating centrally nucleated myofibers and persistence of the inflammatory infiltrate. We demonstrated that iNOS is barely expressed in healthy skeletal muscle, but is selectively induced in inflammatory macrophage-infiltrating muscle at early stages after acute injury.

Interestingly, we found that nNOS, the primary isoform of NOS in skeletal muscle, displays an opposite expression profile compared with iNOS. After muscle injury, nNOS almost completely disappears and is only again detectable at late time points of the regeneration process. Notably, NO plays a nonredundant role in muscle repair after injury by promoting activation, differentiation, and fusion of myogenic precursor cells (10, 29–34). Thus, a source of NO appears necessary for an efficient muscle repair. The present study identifies iNOS, expressed by infiltrating macrophages, as the isoform that provides this NO in the early phases of muscle regeneration. We found that after muscle damage the increase of double-positive activated $Pax7^{+}MyoD^{+}$ myogenic precursor cells is significantly delayed in iNOS-deficient mice compared with wild-type littermates. Activation and subsequent proliferation and terminal differentiation of these cells drive muscle repair through fusion with damaged muscle fibers or with themselves, to produce new fibers (35, 36). Consistently, in injured muscles of iNOS-deficient mice, the expression of myogenin, a marker of differentiation of these myogenic precursor cells, is significantly lower than in those of wild-type mice. All together, our data suggest a critical role of iNOS-derived NO in muscle regeneration. These results may explain why genetic deletion of nNOS does not impair functional muscle regeneration after myotoxic injury (37).

Our results point to another critical role of iNOS in muscle regeneration: the modulation of the inflammatory response. Several studies indicated that iNOS-derived NO is an important homeostatic regulator of leukocyte recruitment in the inflamed microcirculation, suggesting that one of its functions may be to act as an endogenous anti-inflammatory molecule during ongoing inflammation (38). Accordingly, in several inflammatory models, iNOS-deficient mice have difficulty in resolving the inflammation, and neutrophil infiltration persisted for several days longer than in wild-type mice (39). Interestingly, we found that after muscle damage $iNOS^{-/-}$ mice display a greater accumulation of neutrophils and fewer macrophages. Consistently, comparing damaged muscles and muscle-infiltrating macrophages of iNOS-deficient mice with those of wild-type mice, we found higher expression levels of chemokines associated with neutrophil infiltration, such as MIP-1α, MIP2, and MCP3. Thus, it is likely that these chemokines account for the significant increase of neutrophil accumulation in iNOS-deficient mice. Neutrophils release molecules that may contribute to muscle membrane lysis that follows injury. In vivo neutrophil accumulation in muscle after exercise coincides with disruption in myofibril structure (4), and in the presence of bacterial endotoxin the cytotoxic potential of neutrophils significantly increases, thus resulting in enhanced tissue damage and delayed regeneration (40). As such, neutrophil accumulation in $iNOS^{-/-}$ muscles 1 d after damage may contribute to impaired muscle healing. Of note, genetic disruption of the CXCL16 chemokine pathway results in a persistent and important infiltration of injured muscle by neutrophils, defective homing of macrophages, and severely jeopardized tissue regeneration (41).

Interestingly, we found that, in $iNOS^{-/-}$ injured muscles, macrophage recruitment is delayed, but macrophages persist longer as compared with wild-type counterparts. At 1 and 3 d after damage, $iNOS^{-/-}$ muscles display a decreased macrophage infiltration. Consistently, MCP1, a potent chemoattractant and activator of macrophages, was significantly reduced in damaged muscles and muscle-infiltrating macrophages of $iNOS^{-/-}$ mice. However, at 7 and 15 d after damage, macrophages were still significantly present in the muscles of $iNOS^{-/-}$ mice. Persistence of macrophages could potentially derive from the extended presence of necrotic tissue in $iNOS^{-/-}$ mice. Of note, macrophages are critical to the removal of necrotic tissue (42) and together with myogenic precursors and injured fibers are a source of chemokines (6, 43). Accordingly, another mechanism that may contribute to

$iNOS^{+/+}$ and $iNOS^{-/-}$ mice were collected immediately before and 1, 3, 7, and 10 d after injection of CTX and totally lysated. mRNA levels of IGF-1 (M), IL-10 (N), and TNF-α (O) were quantified by real-time PCR analysis and normalized to 28S mRNA levels. Results are expressed as relative fold changes compared with muscles from undamaged control animals (NT). Values shown are the results of experiments on six animals per group. Statistically significant differences are indicated (ANOVA/*t* test; $iNOS^{-/-}$ versus $iNOS^{+/+}$; $^{\S}p < 0.05$, $^{*}p < 0.05$ versus NT).

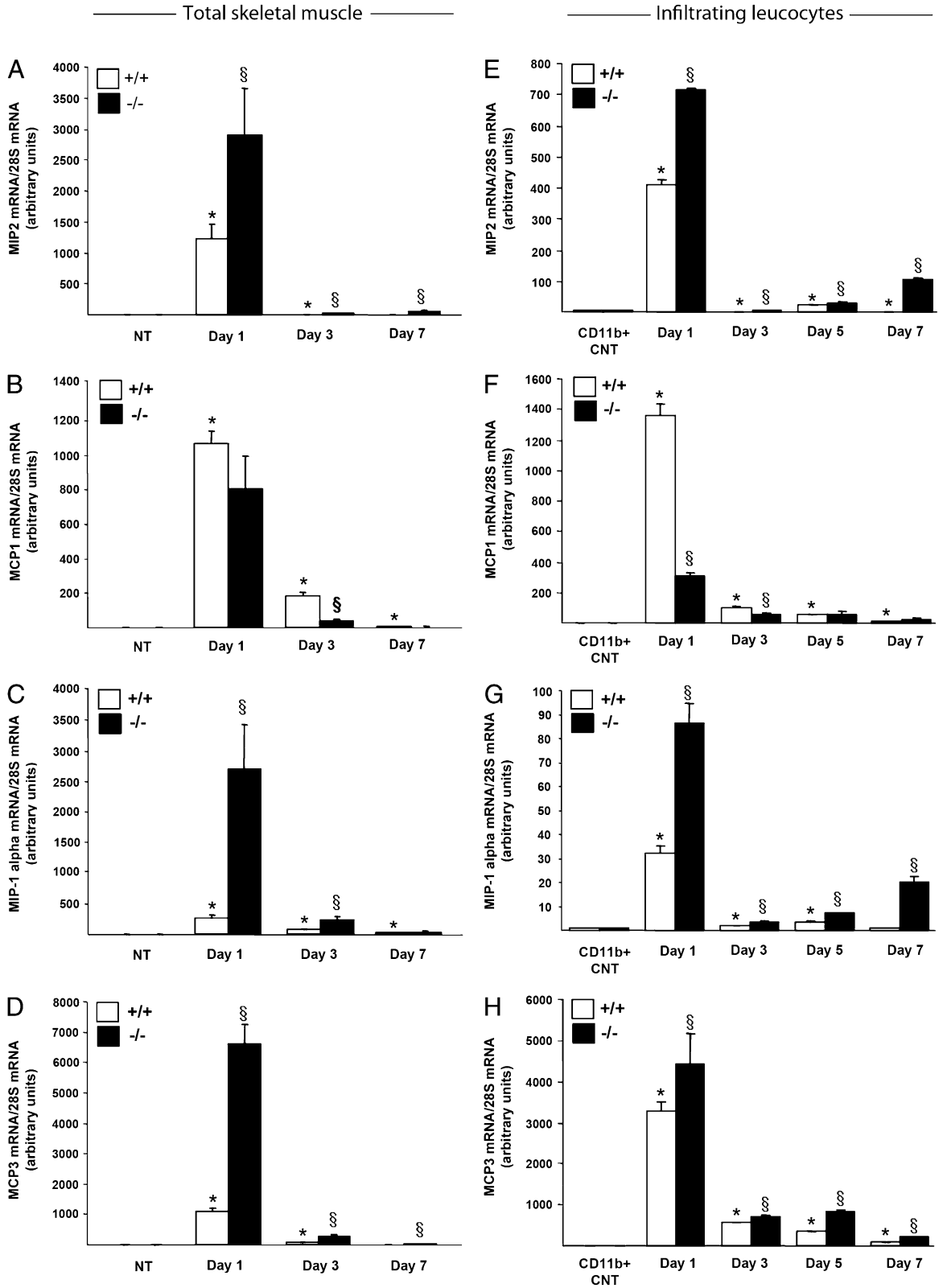

FIGURE 5. Chemokine expression profile in injured iNOS$^{+/+}$ muscles differs from the pattern in the muscles of iNOS$^{-/-}$ mice. Quadriceps and TA muscles from 2-mo-old iNOS$^{+/+}$ and iNOS$^{-/-}$ mice were collected immediately before and 1, 3, 5, and 7 d after injection of CTX. Muscles were totally lysated or digested to isolate CD11b^{+} cells by magnetic bead sorting and processed for RNA extraction. Real-time PCR analyses for MIP2, MCP1, MIP-1α, and MCP3 mRNA expression respectively in total muscle (**A**–**D**) and in muscle-infiltrating CD11b^{+} cells (**E**–**H**) were performed. Results were normalized to 28S mRNA levels and expressed as relative fold changes compared with undamaged muscles (NT) (A–D) or to CD11b^{+} cells retrieved from peripheral blood (CD11b^{+} CNT) (E–H). (A–D) Values shown are the results of experiments on six animals per group. (E–H) Bars indicate the mean ± SD, $n = 3$ mice per three independent experimental cohorts. Statistically significant differences are indicated (ANOVA/t test; iNOS$^{-/-}$ versus iNOS$^{+/+}$; $^{\S}p < 0.05$, $^{*}p < 0.05$ versus NT or CD11b^{+} CNT).

the persistence of macrophages includes alterations in the production of macrophage chemoattractants in the iNOS$^{-/-}$ damaged muscles. Support for this possibility derives from the significantly elevated MIP-1α and MCP3 levels in iNOS$^{-/-}$ macrophage-infiltrating muscle at 5 and 7 d after damage. To our knowledge, these findings provide the first evidence that in damaged muscle iNOS-derived NO can act as a homeostatic regulator of inflammatory leukocyte recruitment.

In conclusion, to our knowledge, we provide the first evidence of a critical role of iNOS in muscle regeneration. Our results identify iNOS-derived NO as a key messenger in regulating myogenic precursor cell fate and the inflammatory response in a model of muscle damage/regeneration, thus revealing a novel mechanism of inflammation-dependent muscle healing. This information may be used to finely tune therapies based on NO donation and regulation of inflammation that appear to be effective in healing muscle damage after acute or prolonged injury (44–47).

Disclosures

The authors have no financial conflicts of interest.

References

1. Chargé, S. B., and M. A. Rudnicki. 2004. Cellular and molecular regulation of muscle regeneration. *Physiol. Rev.* 84: 209–238.
2. Paulsen, G., R. Crameri, H. B. Benestad, J. G. Fjeld, L. Mørkrid, J. Hallén, and T. Raastad. 2010. Time course of leukocyte accumulation in human muscle after eccentric exercise. *Med. Sci. Sports Exerc.* 42: 75–85.
3. Douglas, M. R., K. E. Morrison, M. Salmon, and C. D. Buckley. 2002. Why does inflammation persist: a dominant role for the stromal microenvironment? *Expert Rev. Mol. Med.* 4: 1–18.
4. Fielding, R. A., T. J. Manfredi, W. Ding, M. A. Fiatarone, W. J. Evans, and J. G. Cannon. 1993. Acute phase response in exercise. III. Neutrophil and IL-1 beta accumulation in skeletal muscle. *Am. J. Physiol.* 265: R166–R172.
5. Nguyen, H. X., A. J. Lusis, and J. G. Tidball. 2005. Null mutation of myeloperoxidase in mice prevents mechanical activation of neutrophil lysis of muscle cell membranes in vitro and in vivo. *J. Physiol.* 565: 403–413.
6. Chazaud, B., C. Sonnet, P. Lafuste, G. Bassez, A. C. Rimaniol, F. Poron, F. J. Authier, P. A. Dreyfus, and R. K. Gherardi. 2003. Satellite cells attract monocytes and use macrophages as a support to escape apoptosis and enhance muscle growth. *J. Cell Biol.* 163: 1133–1143.
7. Tidball, J. G., and M. Wehling-Henricks. 2007. Macrophages promote muscle membrane repair and muscle fibre growth and regeneration during modified muscle loading in mice in vivo. *J. Physiol.* 578: 327–336.
8. Brunelli, S., and P. Rovere-Querini. 2008. The immune system and the repair of skeletal muscle. *Pharmacol. Res.* 58: 117–121.
9. Tidball, J. G., and S. A. Villalta. 2010. Regulatory interactions between muscle and the immune system during muscle regeneration. *Am. J. Physiol. Regul. Integr. Comp. Physiol.* 298: R1173–R1187.
10. De Palma, C., and E. Clementi. 2012. Nitric oxide in myogenesis and therapeutic muscle repair. *Mol. Neurobiol.* 46: 682–692.
11. Filippin, L. I., A. J. Moreira, N. P. Marroni, and R. M. Xavier. 2009. Nitric oxide and repair of skeletal muscle injury. *Nitric Oxide* 21: 157–163.
12. Stamler, J. S., and G. Meissner. 2001. Physiology of nitric oxide in skeletal muscle. *Physiol. Rev.* 81: 209–237.
13. Nisoli, E., E. Clementi, M. O. Carruba, and S. Moncada. 2007. Defective mitochondrial biogenesis: a hallmark of the high cardiovascular risk in the metabolic syndrome? *Circ. Res.* 100: 795–806.
14. Buono, R., C. Vantaggiato, V. Pisa, E. Azzoni, M. T. Bassi, S. Brunelli, C. Sciorati, and E. Clementi. 2012. Nitric oxide sustains long-term skeletal muscle regeneration by regulating fate of satellite cells via signaling pathways requiring Vangl2 and cyclic GMP. *Stem Cells* 30: 197–209.
15. Silvagno, F., H. Xia, and D. S. Bredt. 1996. Neuronal nitric-oxide synthase-mu, an alternatively spliced isoform expressed in differentiated skeletal muscle. *J. Biol. Chem.* 271: 11204–11208.
16. Filippin, L. I., M. J. Cuevas, E. Lima, N. P. Marroni, J. Gonzalez-Gallego, and R. M. Xavier. 2011. Nitric oxide regulates the repair of injured skeletal muscle. *Nitric Oxide* 24: 43–49.
17. Filippin, L. I., M. J. Cuevas, E. Lima, N. P. Marroni, J. Gonzalez-Gallego, and R. M. Xavier. 2011. The role of nitric oxide during healing of trauma to the skeletal muscle. *Inflamm. Res.* 60: 347–356.
18. Vezzoli, M., P. Castellani, G. Corna, A. Castiglioni, L. Bosurgi, A. Monno, S. Brunelli, A. A. Manfredi, A. Rubartelli, and P. Rovere-Querini. 2011. High-mobility group box 1 release and redox regulation accompany regeneration and remodeling of skeletal muscle. *Antioxid. Redox Signal.* 15: 2161–2174.
19. Pessina, P., V. Conti, R. Tonlorenzi, T. Touvier, R. Meneveri, G. Cossu, and S. Brunelli. 2012. Necdin enhances muscle reconstitution of dystrophic muscle by vessel-associated progenitors, by promoting cell survival and myogenic differentiation. *Cell Death Differ.* 19: 827–838.
20. Wiendl, H., R. Hohlfeld, and B. C. Kieseier. 2005. Immunobiology of muscle: advances in understanding an immunological microenvironment. *Trends Immunol.* 26: 373–380.
21. Robertson, T. A., M. A. Maley, M. D. Grounds, and J. M. Papadimitriou. 1993. The role of macrophages in skeletal muscle regeneration with particular reference to chemotaxis. *Exp. Cell Res.* 207: 321–331.
22. McLennan, I. S. 1996. Degenerating and regenerating skeletal muscles contain several subpopulations of macrophages with distinct spatial and temporal distributions. *J. Anat.* 188: 17–28.
23. Warren, G. L., T. Hulderman, D. Mishra, X. Gao, L. Millecchia, L. O'Farrell, W. A. Kuziel, and P. P. Simeonova. 2005. Chemokine receptor CCR2 involvement in skeletal muscle regeneration. *FASEB J.* 19: 413–415.
24. Summan, M., G. L. Warren, R. R. Mercer, R. Chapman, T. Hulderman, N. Van Rooijen, and P. P. Simeonova. 2006. Macrophages and skeletal muscle regeneration: a clodronate-containing liposome depletion study. *Am. J. Physiol. Regul. Integr. Comp. Physiol.* 290: R1488–R1495.
25. Arnold, L., A. Henry, F. Poron, Y. Baba-Amer, N. van Rooijen, A. Plonquet, R. K. Gherardi, and B. Chazaud. 2007. Inflammatory monocytes recruited after skeletal muscle injury switch into antiinflammatory macrophages to support myogenesis. *J. Exp. Med.* 204: 1057–1069.
26. Villalta, S. A., C. Rinaldi, B. Deng, G. Liu, B. Fedor, and J. G. Tidball. 2011. Interleukin-10 reduces the pathology of mdx muscular dystrophy by deactivating M1 macrophages and modulating macrophage phenotype. *Hum. Mol. Genet.* 20: 790–805.
27. Segawa, M., S. Fukada, Y. Yamamoto, H. Yahagi, M. Kanematsu, M. Sato, T. Ito, A. Uezumi, S. Hayashi, Y. Miyagoe-Suzuki, et al. 2008. Suppression of macrophage functions impairs skeletal muscle regeneration with severe fibrosis. *Exp. Cell Res.* 314: 3232–3244.
28. Ruffell, D., F. Mourkioti, A. Gambardella, P. Kirstetter, R. G. Lopez, N. Rosenthal, and C. Nerlov. 2009. A CREB-C/EBPbeta cascade induces M2 macrophage-specific gene expression and promotes muscle injury repair. *Proc. Natl. Acad. Sci. USA* 106: 17475–17480.
29. Anderson, J. E. 2000. A role for nitric oxide in muscle repair: nitric oxide-mediated activation of muscle satellite cells. *Mol. Biol. Cell* 11: 1859–1874.
30. Tatsumi, R., X. Liu, A. Pulido, M. Morales, T. Sakata, S. Dial, A. Hattori, Y. Ikeuchi, and R. E. Allen. 2006. Satellite cell activation in stretched skeletal muscle and the role of nitric oxide and hepatocyte growth factor. *Am. J. Physiol. Cell Physiol.* 290: C1487–C1494.
31. Betters, J. L., J. H. Long, K. S. Howe, R. W. Braith, Q. A. Soltow, V. A. Lira, and D. S. Criswell. 2008. Nitric oxide reverses prednisolone-induced inactivation of muscle satellite cells. *Muscle Nerve* 37: 203–209.
32. Pisconti, A., S. Brunelli, M. Di Padova, C. De Palma, D. Deponti, S. Baesso, V. Sartorelli, G. Cossu, and E. Clementi. 2006. Follistatin induction by nitric oxide through cyclic GMP: a tightly regulated signaling pathway that controls myoblast fusion. *J. Cell Biol.* 172: 233–244.
33. De Palma, C., S. Falcone, S. Pisoni, S. Cipolat, C. Panzeri, S. Pambianco, A. Pisconti, R. Allevi, M. T. Bassi, G. Cossu, et al. 2010. Nitric oxide inhibition of Drp1-mediated mitochondrial fission is critical for myogenic differentiation. *Cell Death Differ.* 17: 1684–1696.
34. Colussi, C., C. Mozzetta, A. Gurtner, B. Illi, J. Rosati, S. Straino, G. Ragone, M. Pescatori, G. Zaccagnini, A. Antonini, et al. 2008. HDAC2 blockade by nitric oxide and histone deacetylase inhibitors reveals a common target in Duchenne muscular dystrophy treatment. *Proc. Natl. Acad. Sci. USA* 105: 19183–19187.
35. Cossu, G., and S. Biressi. 2005. Satellite cells, myoblasts and other occasional myogenic progenitors: possible origin, phenotypic features and role in muscle regeneration. *Semin. Cell Dev. Biol.* 16: 623–631.
36. Zammit, P. S., F. Relaix, Y. Nagata, A. P. Ruiz, C. A. Collins, T. A. Partridge, and J. R. Beauchamp. 2006. Pax7 and myogenic progression in skeletal muscle satellite cells. *J. Cell Sci.* 119: 1824–1832.
37. Church, J. E., S. M. Gehrig, A. Chee, T. Naim, J. Trieu, G. K. McConell, and G. S. Lynch. 2011. Early functional muscle regeneration after myotoxic injury in mice is unaffected by nNOS absence. *Am. J. Physiol. Regul. Integr. Comp. Physiol.* 301: R1358–R1366.
38. Hickey, M. J., K. A. Sharkey, E. G. Sihota, P. H. Reinhardt, J. D. Macmicking, C. Nathan, and P. Kubes. 1997. Inducible nitric oxide synthase-deficient mice have enhanced leukocyte-endothelium interactions in endotoxemia. *FASEB J.* 11: 955–964.
39. McCafferty, D. M., J. S. Mudgett, M. G. Swain, and P. Kubes. 1997. Inducible nitric oxide synthase plays a critical role in resolving intestinal inflammation. *Gastroenterology* 112: 1022–1027.
40. Dumont, N., P. Bouchard, and J. Frenette. 2008. Neutrophil-induced skeletal muscle damage: a calculated and controlled response following hindlimb unloading and reloading. *Am. J. Physiol. Regul. Integr. Comp. Physiol.* 295: R1831–R1838.
41. Zhang, L., L. Ran, G. E. Garcia, X. H. Wang, S. Han, J. Du, and W. E. Mitch. 2009. Chemokine CXCL16 regulates neutrophil and macrophage infiltration into injured muscle, promoting muscle regeneration. *Am. J. Pathol.* 175: 2518–2527.
42. Tidball, J. G. 1995. Inflammatory cell response to acute muscle injury. *Med. Sci. Sports Exerc.* 27: 1022–1032.
43. Lu, H., D. Huang, R. M. Ransohoff, and L. Zhou. 2011. Acute skeletal muscle injury: CCL2 expression by both monocytes and injured muscle is required for repair. *FASEB J.* 25: 3344–3355.
44. Sciorati, C., R. Buono, E. Azzoni, S. Casati, P. Ciuffreda, G. D'Angelo, D. Cattaneo, S. Brunelli, and E. Clementi. 2010. Co-administration of ibuprofen and nitric oxide is an effective experimental therapy for muscular dystrophy, with immediate applicability to humans. *Br. J. Pharmacol.* 160: 1550–1560.

45. Sciorati, C., D. Miglietta, R. Buono, V. Pisa, D. Cattaneo, E. Azzoni, S. Brunelli, and E. Clementi. 2011. A dual acting compound releasing nitric oxide (NO) and ibuprofen, NCX 320, shows significant therapeutic effects in a mouse model of muscular dystrophy. *Pharmacol. Res.* 64: 210–217.
46. Brunelli, S., C. Sciorati, G. D'Antona, A. Innocenzi, D. Covarello, B. G. Galvez, C. Perrotta, A. Monopoli, F. Sanvito, R. Bottinelli, et al. 2007. Nitric oxide release combined with nonsteroidal antiinflammatory activity prevents muscular dystrophy pathology and enhances stem cell therapy. *Proc. Natl. Acad. Sci. USA* 104: 264–269.
47. D'Angelo, M. G., S. Gandossini, F. Martinelli Boneschi, C. Sciorati, S. Bonato, E. Brighina, G. P. Comi, A. C. Turconi, F. Magri, G. Stefanoni, et al. 2012. Nitric oxide donor and non steroidal anti inflammatory drugs as a therapy for muscular dystrophies: evidence from a safety study with pilot efficacy measures in adult dystrophic patients. *Pharmacol. Res.* 65: 472–479.